HVMUX, a high voltage multiplexing for the ATLAS Tracker upgrade

Published by IOP Publishing for Sissa Medialab

Received: *December 7, 2016*
Accepted: *January 12, 2017*
Published: *January 25, 2017*

14TH Topical Seminar on Innovative Particle and Radiation Detectors
3–6 October 2016
Siena, Italy

HVMUX, a high voltage multiplexing for the ATLAS Tracker upgrade

E. Giulio Villani,[a,1] **P. Phillips,**[a] **J. Matheson,**[a] **Z. Zhang,**[a] **D. Lynn,**[b] **P. Kuczewski,**[b] **L.B.A. Hommels,**[c] **I. Gregor,**[d] **M. Bessner,**[d] **K. Tackmann,**[d] **F.M. Newcomer,**[e] **E. Spencer**[f] **and A. Greenall**[g]

[a] *STFC Rutherford Appleton Laboratory Particle Physics Dept., STFC Rutherford Appleton Laboratory , Harwell, Didcot, OX110QX, U.K.*
[b] *Brookhaven National Laboratory (BNL), Upton, NY 11973 (NY), U.S.A.*
[c] *Cavendish Laboratory, University of Cambridge, JJ Thomson Ave, Cambridge CB3 0HE, U.K.*
[d] *Deutsches Elektronen Synchrotron (DESY), Notkestraße 85, 22607 Hamburg, Germany*
[e] *University of Pennsylvania, 209 S 33rd St, Philadelphia, PA 19104, U.S.A.*
[f] *University of California Santa Cruz (SCIPP-UCSC), 1156 High Street, Santa Cruz, CA 95064, U.S.A.*
[g] *Oliver Lodge Laboratory, The University of Liverpool, Cambridge St, Liverpool L69 7ZE, U.K.*

E-mail: giulio.villani@stfc.ac.uk

Abstract: The HV biasing solution adopted in the current ATLAS detector uses one HV conductor for each sensor. This approach easily allows disabling of malfunctioning sensors without affecting the others, but space constraints and material budget considerations renders this approach impractical for the Upgraded detector. In fact, the increased luminosity of the Upgraded LHC will require more channels in the upgraded ATLAS Tracker, as a result of the finer detector segmentation. Different approaches to bring the HV biasing to the detectors, including the use of a shared HV line to bias several sensors and employing semiconductor switches for the HV routing (HVMUX), have been investigated. Beside the size constraints, particular attention must be paid to the radiation tolerance of any proposed solution, which, for the strips detector, requires proper operation up to

[1] Corresponding author.

doi:10.1088/1748-0221/12/01/C01076

fluences of the order of $2 \cdot 10^{15}$ 1MeV n_{eq}/cm^2 and TID in excess of 300 kGy. In this paper, a description of the proposed HVMUX solution, along with electrical and radiation tests results will be presented and discussed.

KEYWORDS: Radiation-hard electronics; Voltage distributions

Contents

1 Introduction

The high voltage powering approach implemented in the current Semiconductor Tracker system (SCT), one of the three sub-detectors of the present ATLAS tracker, consists of individual high voltage biasing to the strip sensors by means of individual power supplies, which are remotely located in a service cavern [1, 2].

Such one-to-one approach guarantees optimal robustness to the biasing system, as it allows individual disabling of malfunctioning sensors without disturbing the others. The monitoring of the individual current drawn by each sensor is also greatly simplified, an important requisite to assess their proper functioning.

To fulfill the requirements of the High Luminosity upgrade of the Large Hadron Collider (HL-LHC) [3, 4], the ATLAS Tracker Upgrade will consist of an all silicon tracking detector. For the strip barrel, the adopted baseline solution relies on the stave concept, figure 1. On each side of the stave barrel up to 14 single-sided silicon strip detector modules are glued directly to each side of the support carbon fibre structure, which embeds the cooling pipe. The routing of signals and power between the modules and the End Of Stave (EoS) board, that acts as interface to the stave and is located at one end of the stave, is provided by a long kapton flex circuit, known as Bus Tape, that is glued to the carbon fibre skin of the stave.

However, in the Tracker Upgrade, the increased number of sensors will not allow to implement the individual biasing approach: lack of space for cables and constraints on material budget will not permit each sensor to have its own HV bias [5]. For example, if existing cables are re-used, groups of 4 sensors or more will have to be connected in parallel. This solution would satisfy the space and constraints on material budget but could lead to the loss of the other modules on the same bias line, should one sensor fail due to high current.

To avoid such potential losses, a solution has been investigated that consists of having a number of modules on each side of the stave biased by a single HV line but with each sensor that can be disconnected from the HV bias line through a detector slow control link (DCS) acting on a high voltage switch (HVMUX).

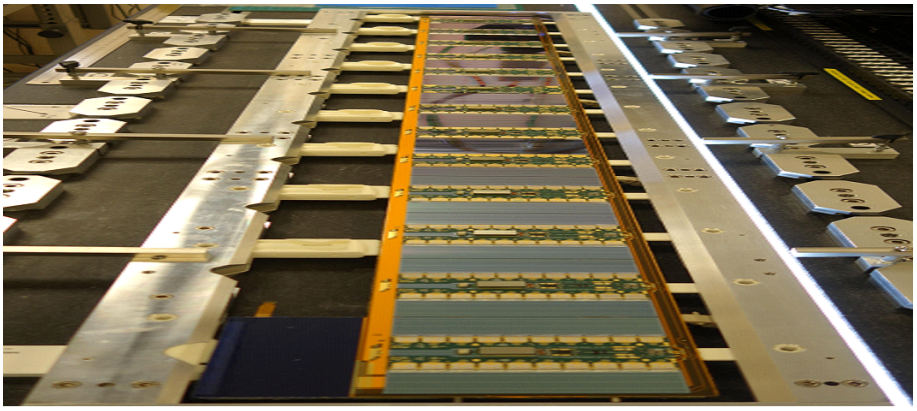

Figure 1. A complete strip stave assembled at RAL.

In this paper, section 2 will give a description of the HVMUX system, along with details of required technical specifications and size constraints. In section 3 a detailed description of the implemented HVMUX circuitry along with test results will be provided. In section 4 a description of neutron irradiation test performed on HVMUX components and related test results will be given. Finally, in section 5, conclusions and next steps of the development of this project will be provided.

2 HVMUX description

A schematic diagram of the HVMUX approach is shown in figure 2. Each one of the HV switches is individually addressable through DCS signal and permits enabling or disabling of the HV biasing to a strip sensor.

The operating environment of ATLAS Tracker Upgrade demands challenging requirements for the HV switches. When disabled, the HV switches should be able to withstand in excess of 500 V, at the same time exhibiting low leakage current, much smaller than the leakage current of the sensors (few 100's nA when non irradiated and increasing up to ~mA's after 10 years of operation). Conversely, when enabled, the switches should present a relatively low resistance, to allow the flow of current up to a few mA's without adding a significant voltage drop along the bias line.

The predictions for the maximum neutron fluence and dose of ionizing radiation in the strip barrel detectors are $5.3 \cdot 10^{14}$ 1MeV n_{eq}/cm^2, 216 kGy for the short strips in layer 1 and $8.1 \cdot 10^{14}$ 1MeV n_{eq}/cm^2, 288 kGy for the strip end cap [6]. A specification of $2{\cdot}10^{15}$ 1MeV n_{eq}/cm^2 and TID of 60 Mrad(Si) is therefore imposed to allow for uncertainties in fluence calculations, which sets the targeted radiation tolerance of the HV switches. Moreover, the HV switches should be able to operate in a strong magnetic field of around 2 T, at low temperature and, finally, represent an economically viable solution, as the number of devices needed will be in excess of 10,000.

Currently, the allocated area for the implementation of the HVMUX circuitry is on the hybrid of the strip module, figure 3, where a 'power board' PCB carrier would include the LV powering, the HVMUX circuitry and the current measuring circuitry. The total available circuit area is therefore limited to 6×9 mm^2.

2017 JINST 12 C01076

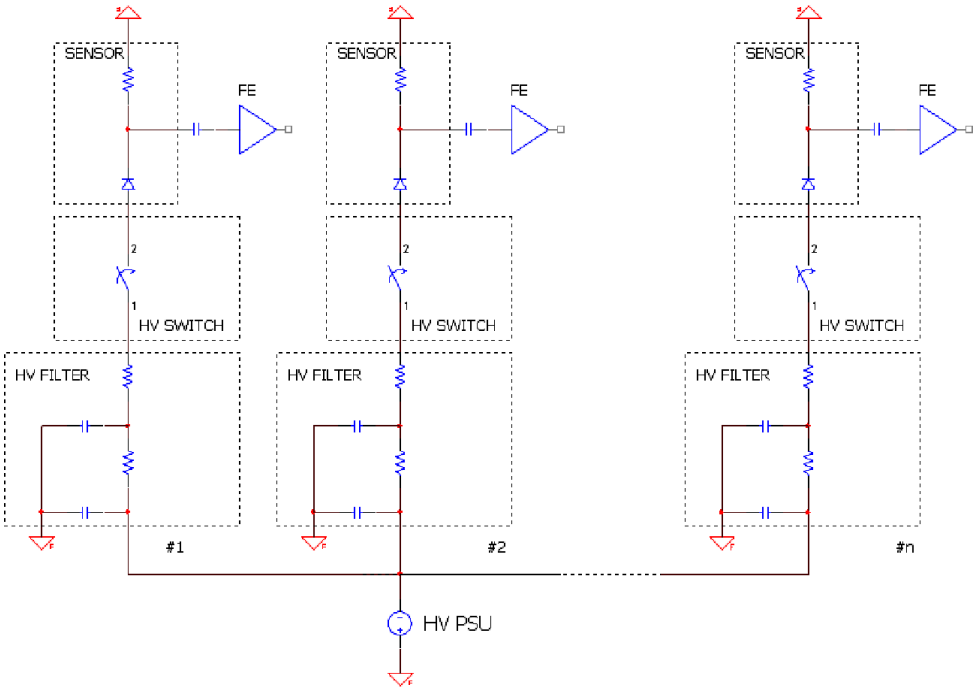

Figure 2. A simplified HVMUX schematic diagram. The HV switches share the common low side of the HV bias. The enabling of the HV switches is done via a DCS signal (not shown in the diagram).

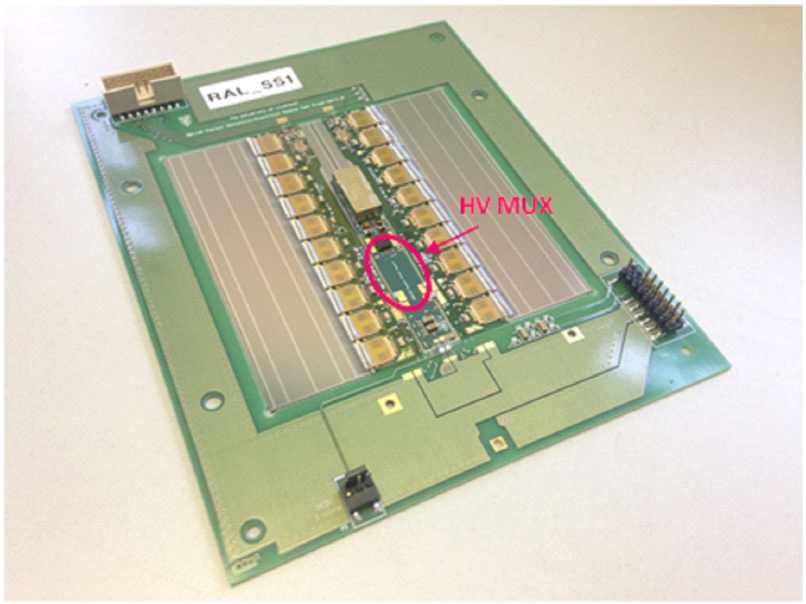

Figure 3. A barrel stave module. On the hybrid, the power board will include the DC to DC LV and HVMUX section. The allocated area for the HV MUX implementation is highlighted.

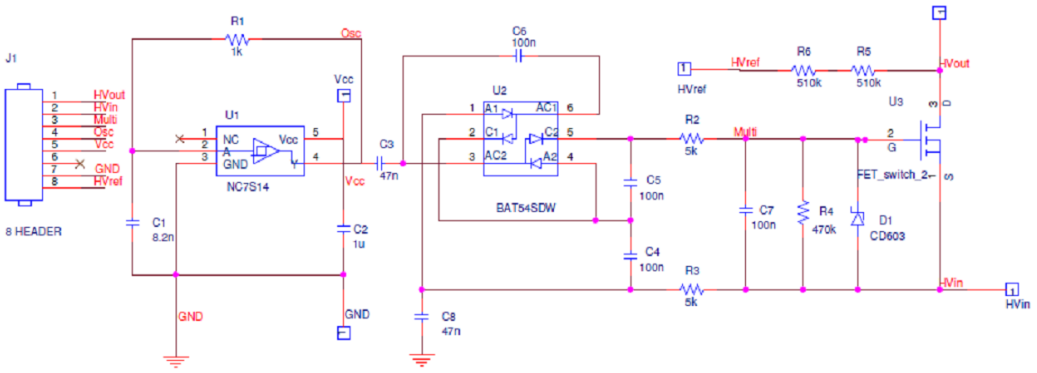

Figure 4. The schematic diagram of the tested HVMUX circuitry. The AC signal is provided by a Schmitt trigger oscillator, which will be included in the AMAC ASIC. The HV supply is applied to the HV_{in} node, the load to the HV_{out} node. The component C8 is needed only in case of alternative solution employing a Silicon-based n-JFET HV device, currently under development. It is not used in the test described here.

3 HVMUX implementation and tests results

A circuit schematic and PCB implementation of a HV switch which fulfils the size requirements outlined above for the HVMUX are shown in figure 4 and 5. The circuit consists of an AC-coupled Greinacher voltage multiplier that employs Schottky diodes as rectifying elements, followed by a low pass filter to drive the gate of a normally-off GaN FET device rated for high voltage, a Panasonic PGA26E19B.

The AC-coupled approach allows decoupling of the high voltage nodes of the switch circuit from the low voltage nodes of the hybrid and effectively requires just one control line, carrying the AC signal, for its operation. With the values shown, by applying a square wave AC voltage of 2 V amplitude to the coupling capacitor C3, a DC voltage of around 2.5 V is generated across the gate of the GaN device, sufficiently high to turn it fully on, which allows the HV bias to be applied to the load, figure 6. Conversely, by stopping the AC signal, the GaN device is turned off which in turn stops the HV bias, figure 7. The Zener diode placed across the gate of the GaN device protects against overvoltage that could damage the device. The AC voltage frequency is set to a nominal 100 kHz to reduce ripple on the DC output. The currently being designed Autonomous Monitor and Control (AMAC) ASIC, which will be integral part of the power board of the strips hybrids, [7], will include this AC voltage generation section, further reducing the total area required by the HVMUX circuitry.

The maximum voltage operation of the proposed circuitry depends on the maximum voltage rating of the GaN device, albeit a stacked devices solution would allow achieving higher voltage capabilities [8], and of the coupling capacitor C3. Therefore, such solution could be employed for the HV biasing of sensor requiring even higher voltages than those presented here.

In order to verify the suitability of this approach, all the components used in this HVMUX implementation had to be tested for radiation hardness, to confirm their reliability under the stringent operating conditions defined above.

2017 JINST 12 C01076

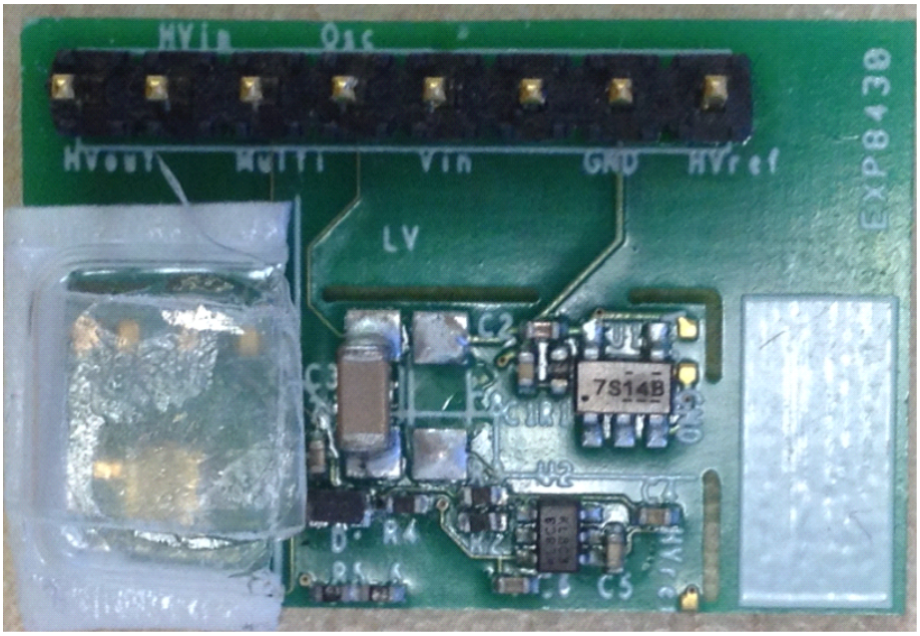

Figure 5. Implementation of the above schematic on a PCB board. The edge connector has been added for stand-alone test of the board. The cut-out board has the required size to fit in the allocated space on the module hybrid. The HV GaN device, of 2×2 mm^2 footprint, is on the left, under a plastic cover for wire bonds protection.

4 Devices description and neutron tests results

The challenging requirements for the HV switches outlined above made it impossible to identify readily available silicon devices suitable for this application. Silicon based HV voltage devices tend to show high sensitivity to both ionizing and non-ionizing radiation, either due to the presence of thick silicon dioxide layer (MOS), resulting in excessive threshold voltage shift, or type of doping (n-JFET), resulting in excessive increase of resistance and/or leakage current after irradiation up to the dose levels indicated above [9–11].

A number of devices, based upon wide band gap material, including SiC and GaN, have been investigated to assess their suitability to this task. Some initial results are reported in previous papers [8].The radiation resistance of such devices is expected to be higher compared to silicon based ones, essentially owing to their higher average displacement energy threshold, stemming from their bigger unit cell size [12].

Recent tests were carried out on GaN based devices rated for high voltage and used in the HVMUX circuitry described in section 3, using the neutron irradiation facility available at the JSA TRIGA reactor [13]. For this purpose, a system capable of measuring in real time the devices characteristics was set up and used for the test, figure 8. The system, which consists of a Keithley 7002 switch control mainframe unit housing a 7154 low voltage and 7011 high voltage switch cards, all controlled by a dedicated Labview program, allows HV biasing and current measuring of up to ten devices at once during the irradiation, so as to monitor and record their parameter changes at various levels of neutron fluence. A number of GaN and Si devices were irradiated up to neutron

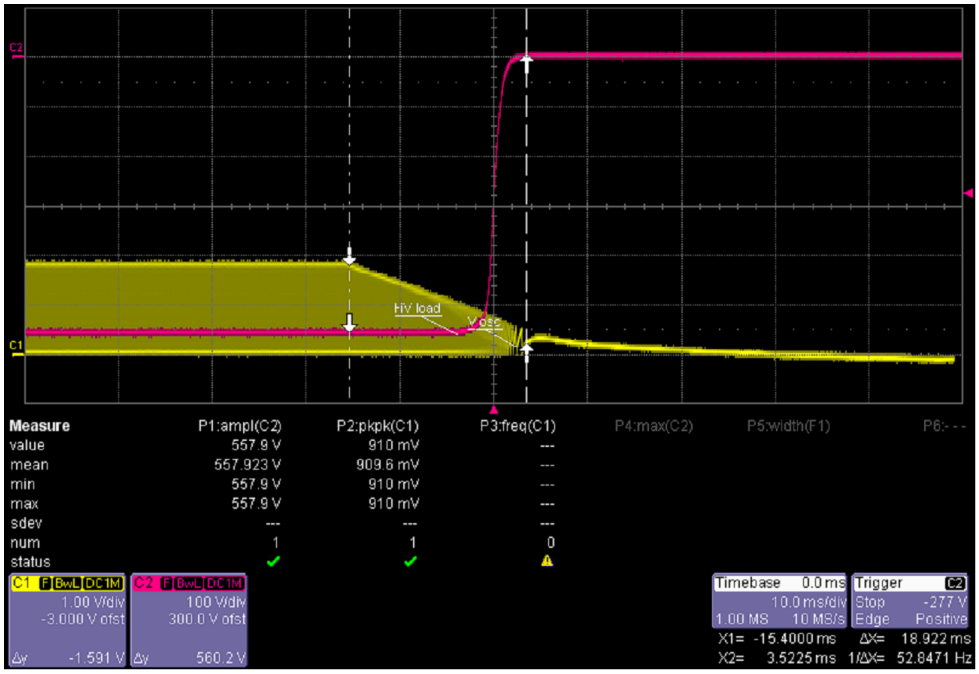

Figure 6. Example plot of transition from HV bias ON (−550 V) to 0 V. When the powering to the oscillator is turned off, its output (yellow track) drops, turning the GaN device off. This quickly sets the potential of the HVout node (red track) to ground. The load used in this test was a 50 kOhm resistor, to emulate the maximum current drawn by an irradiated sensor. The leakage current measured through the GaN in the OFF state is around 60 nA.

fluences in excess of 10^{16} cm^{-2}, using the TIC irradiation channel, the neutron energy spectrum of which, figure 9, closely resembles the expected neutron energy spectrum of the upgraded ATLAS tracker strip barrel [14].

During the radiation tests the GaN devices were alternately kept in the off state, with $V_{gs} = 0$ V and biased at high voltage, with $V_{ds} = 550$ V, to measure their leakage current, and then turned on, $V_{gs} = 2$ V and biased with $I_{ds} = 10$ mA current, to measure their resistance increase. Results of the radiation tests for the increase in resistance in the on state for the EPC2027 and PGA26E19BV devices are shown in figure 10 and 11 respectively. Results of the radiation tests for the increase in leakage current at high voltage bias for the EPC2027 and PGA26E19BV devices are shown in figure 12 and 13.

The tested samples of HV GaN devices showed negligible changes in conductivity in the on state, which is the nominal operating condition of the devices in the proposed project. More relevant changes are observed in the threshold voltage of the devices, particularly for the EPC2027, whilst in the case of the PGA26E19BV these are more reduced. The differences observed in threshold voltage shifts direction between the two types of GaN devices can probably be attributed to different sensitivity to defects arising from differences in device structure.

A number of Si based devices, including Schottky and Zener diodes needed in the HVMUX circuitry, were also irradiated 'passively', i.e. without online monitoring, by placing them in a plastic container dropped in the TIC channel of the reactor, and exposed to a maximum neutron fluence

2017 JINST 12 C01076

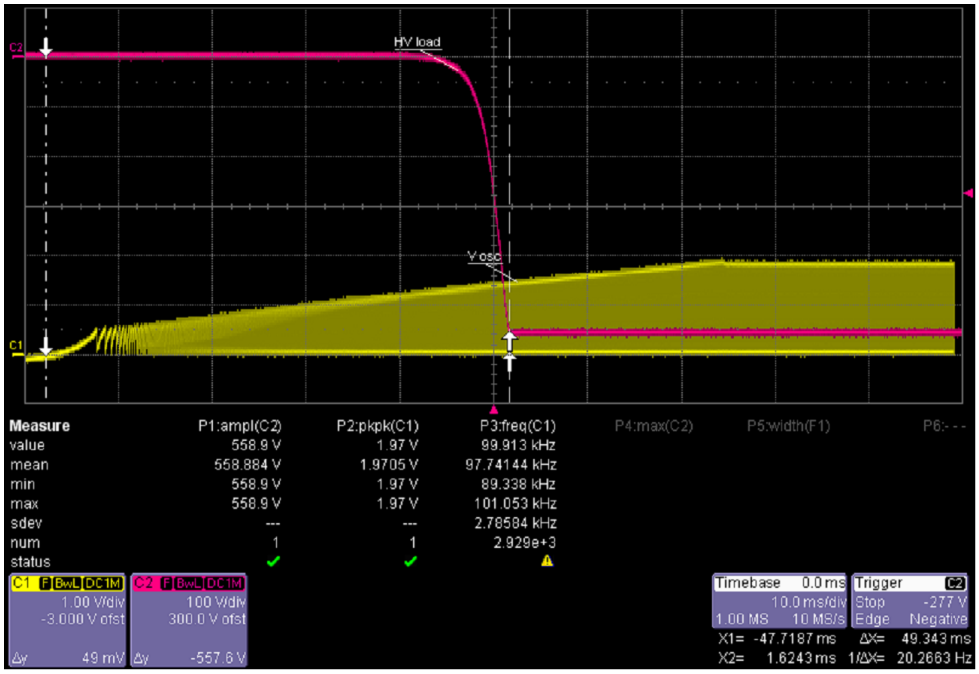

Figure 7. Example plot of transition from HV bias OFF (0 V) to ON (−550 V). When the powering to the oscillator is turned on, its AC output (yellow track) increases until the GaN device is turned on. This quickly sets the potential of the HVout node (red track) to its nominal bias value. The residual voltage across the GaN device when in the ON state, with an Ids current of 10 mA, is around 50 mV.

of $6 \cdot 10^{15}$ cm^{-2}. The devices were then characterized for changes after their residual radiation activity dropped to background level. Test results of irradiation of Schottky and Zener diodes are shown in figure 14 and 15 respectively. Minor changes were observed in the characteristics of the Schottky diodes, predominantly in the forward bias region, whilst the leakage current in the reverse region is practically unchanged from the non-irradiated case. The Zener diodes tested showed more pronounced variations in their characteristics, both in the forward and reverse region. Nonetheless, the changes in characteristics are still small enough not to affect their intended use in this project.

5 Conclusions

HVMUX is the approach currently being pursued to distribute the HV in the ATLAS Tracker upgrade. It consists of sharing the HV line among several sensors connected in parallel. To guarantee an acceptable level of robustness, each sensor will have to be equipped with a HV switch, to avoid impairment of the functioning of the other sensors connected in parallel. A dedicated circuitry for the HVMUX implementation has been designed, fabricated and tested. Tests on staves will be carried out soon.

The devices used in the circuit have been tested for their radiation hardness with neutrons to fluences in excess of $6 \cdot 10^{15}$ 1MeV n_{eq}/cm^2 and found to be still fully functional. Tests on a higher number of devices and with different types of radiation, including protons, gamma and pions, to confirm their suitability to this task, will be performed soon.

2017 JINST 12 C01076

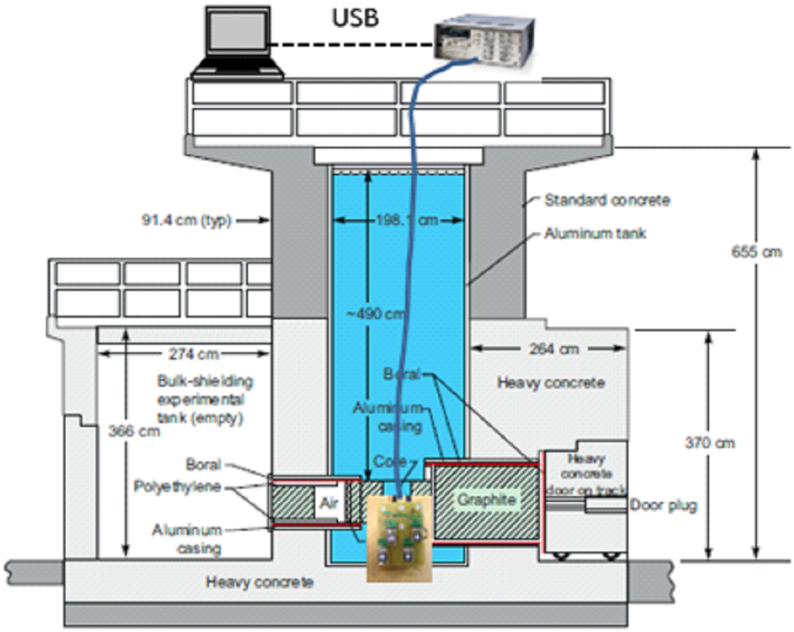

Figure 8. Schematic layout of the test system in the reactor. The board holding the devices is inserted down the TIC channel into the core of the reactor. Power cables connect the devices to the DAQ placed on top of the open pool reactor. At the reactor full power (250 kW), the highest achievable neutron flux can reach approximately $2 \cdot 10^{13}$ cm^{-2}s^{-1}.

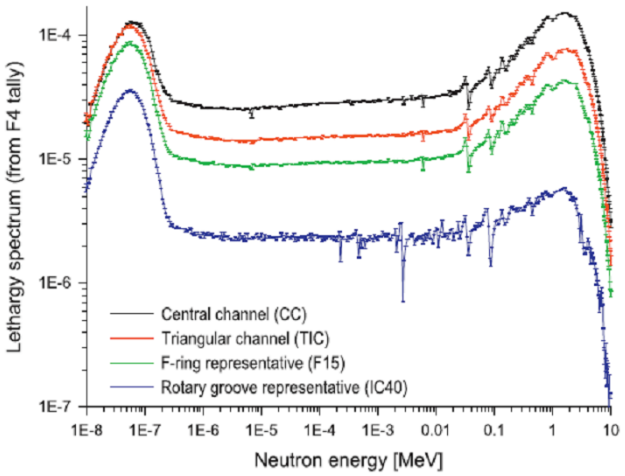

Figure 9. Lethargy neutron spectrum, normalized per source neutron, in some of the irradiation channels. The TIC channel is shown in red. More than 32% of its total neutron flux is in the energy above 100 keV.

Acknowledgments

The authors would like to thank Igor Mandić for his help in the setting up and assistance during the irradiation test at the Jožef Stefan Institute, Ljubljana.

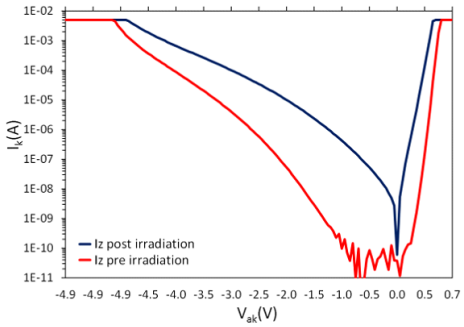

Figure 10. Average changes of V_{ds} and I_{gs} of four EPC2027 devices versus neutron fluence. In the on state, the devices were biased with V_{gs} = 3 V and I_{ds} = 10 mA.

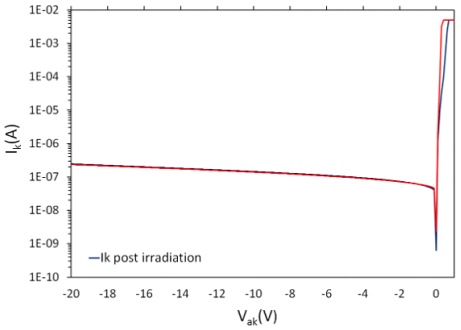

Figure 11. Average changes of V_{ds} and I_{gs} of four PGA26E19BV devices versus neutron fluence. In the on state, the devices were biased with V_{gs} = 2 V and I_{ds} = 10 mA.

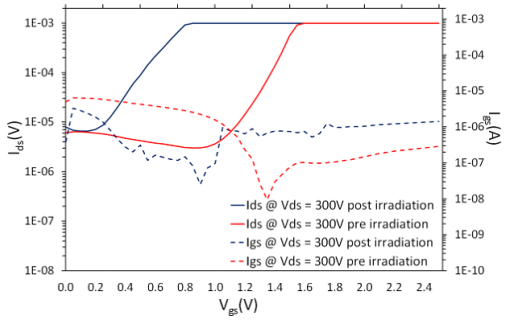

Figure 12. Average I_{ds} and I_{gs} plots versus V_{gs} of four non-irradiated (red) and irradiated to > 10^{-16} n_{eq}/cm^2 (blue) EPC2027 devices. The devices were biased with V_{ds} = 550 V and current compliance set to 1 mA.

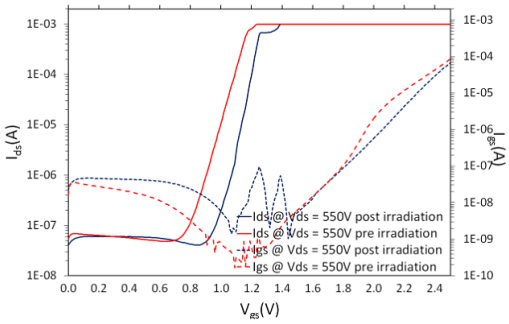

Figure 13. Average I_{ds} and I_{gs} plots versus V_{gs} of four non-irradiated (red) and irradiated to > 10^{-16} n_{eq}/cm^2 (blue) PGA26E19BV devices. The devices were biased with V_{ds} = 550 V and current compliance set to 1 mA.

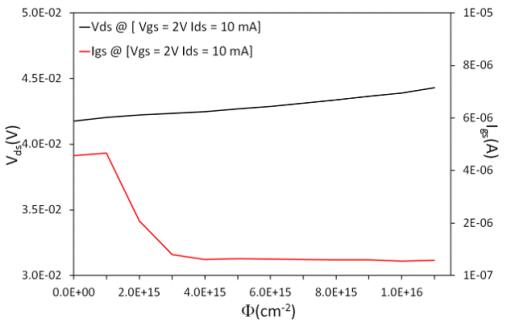

Figure 14. Average I_k versus V_k plots of four non-irradiated (red) and irradiated to $2 \cdot 10^{-15}$ n_{eq}/cm^2 (blue) BAT54SDW Schottky diode devices. Current compliance is set to 5 mA.

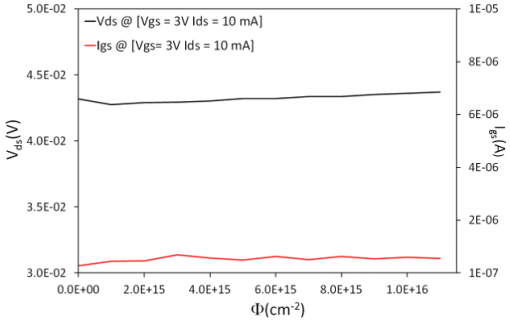

Figure 15. Average I_z versus V_z plots of four non-irradiated (red) and irradiated to $2 \cdot 10^{-15}$ n_{eq}/cm^2 (blue) CD0603 Zener diode devices in the forward and reverse region. Current compliance is set to 5 mA.

2017 JINST 12 C01076

References

[1] P. Phillips, *ATLAS SCT power supply system*, in the proceedings of the *Topical Workshop on Electronics for Particle Physics (TWEPP 2007)*, September 3–7, Prague, Czech Republic (2007) [CERN-2007-00].

[2] J. Bohm et al., *Power supply and power distribution system for the ATLAS silicon strip detectors*, in the proceedings of the 7th *Workshop on Electronics for LHC Experiments*, September 10–14, Stockholm, Sweden (2001) [CERN-2001-005].

[3] A. Clark, M. Elsing and P. Wells, *Performance specifications of the tracker Phase-II upgrade*, ATL-UPGRADE-PUB-2012-003 (2012).

[4] A. Clark et al., *Final report: ATLAS Phase-II tracker upgrade layout task force*, ATL-UPGRADE-PUB-2012-004 (2012).

[5] ATLAS collaboration, *ATLAS letter of intent Phase II upgrade*, CERN-LHCC-2012-022 (2013).

[6] P.S. Miyagawa and I. Dawson, *Radiation background studies for the Phase-II inner tracker upgrade*, ATL-UPGRADE-INT-2012-002 (2012).

[7] ATLAS collaboration, *ATLAS silicon strip electronics*, ATL-UPGRADE-SLIDE-2016-116.

[8] E.G. Villani et al., *HVMUX, the High Voltage Multiplexing for the ATLAS Tracker Upgrade*, 2015 *JINST* **10** C01041.

[9] A. Holmes-Siedle and L. Adams, *Handbook of radiation effects*, 2nd edition, Oxford University Press, Oxford U.K. (2002).

[10] M. Citterio, et al., *A study of low noise JFETs exposed to large doses of gamma rays and neutrons*, *IEEE Nucl. Sci. Symp. Conf. Rec.* **2** (1992) 794.

[11] E.G. Villani et al., *High voltage multiplexing for the ATLAS tracker upgrade*, 2014 *JINST* **9** C01032.

[12] J. Grant et al., *Wide bandgap semiconductors for harsh radiation environments*, *Nucl. Instrum. Meth.* **A 546** (2005) 213.

[13] L. Snoj, G. Zerovnik and A. Trkov, *Computational analysis of irradiation facilities at the JSI TRIGA reactor*, *Appl. Radiat. Isot.* **70** (2012) 483.

[14] https://twiki.cern.ch/twiki/bin/viewauth/Atlas/AtlasUpgrade#Radiation_backgrounds.

2017 JINST 12 C01076